frontiers | Frontiers in Marine Science

TYPE Original Research
PUBLISHED 26 July 2024
DOI 10.3389/fmars.2024.1389673

OPEN ACCESS

EDITED BY
Mahmood Sadat-Noori,
James Cook University, Australia

REVIEWED BY
Yunchao Wu,
Chinese Academy of Sciences (CAS), China
César Megina,
Sevilla University, Spain

*CORRESPONDENCE
Valle Perez-Rodriguez
valle.perez@uca.es

RECEIVED 21 February 2024
ACCEPTED 13 June 2024
PUBLISHED 26 July 2024

CITATION
Perez-Rodriguez V, Corzo A, Papaspyrou S, van Bergeijk SA, Vilas C, Cañavate JP and Garcia-Robledo E (2024) Benthic metabolism and nutrient dynamics of a hyperturbid and hypernutrified estuary.
Front. Mar. Sci. 11:1389673.
doi: 10.3389/fmars.2024.1389673

Benthic metabolism and nutrient dynamics of a hyperturbid and hypernutrified estuary

Valle Perez-Rodriguez[1,2]*, Alfonso Corzo[1,2], Sokratis Papaspyrou[1,2], Stefanie Anne van Bergeijk[3], Cesar Vilas[3], José Pedro Cañavate[3] and Emilio Garcia-Robledo[1,2]

[1]Microbial Ecology and Biogeochemistry Laboratory, Department of Biology, Faculty of Marine and Environmental Science, University of Cadiz, Puerto Real, Spain, [2]Instituto Universitario de Investigación Marina (INMAR), Cadiz, Spain, [3]Acuicultura, Pesca y Medio Marino, Instituto Andaluz de Investigación y Formación Agraria, Pesquera, Alimentaria y de la Producción Ecológica (IFAPA) Centro El Toruño, El Puerto de Santa María, Spain

The biogeochemical role of the sediments in the Guadalquivir River estuary, a vital region in the SW Iberian Peninsula, has been considerably neglected. The benthic microalgae (microphytobenthos, MPB) inhabiting the sediment surface could contribute to the autochthonous primary production and influence nutrient recycling in this hyper-turbid and hypernutrified estuary. Sediment–water column fluxes of O_2 and dissolved inorganic nitrogen species (DIN = NH_4^+ + NO_3^- + NO_2^-) were assessed in laboratory incubations of sediment cores from Bonanza (mouth) and Lebrija (middle) during a 1-year study. Vertical profiles down to the 10-cm depth of photosynthetic pigments, organic C, total nitrogen, DIN, Fe^{2+}, SO_4^{2-}, and dissolved inorganic carbon (DIC) were also measured. Chlorophyll *a* in the sediment surface was higher at the estuarine mouth, exhibiting a seasonal pattern at both sites with highest values in winter and lowest in summer. Net community production (NCP) was higher in Bonanza compared with Lebrija and showed positive values most of the year, indicating that MPB contributed to the overall autochthonous primary production of the estuary. Seasonal changes in chlorophyll *a* and NCP were not parallel, suggesting different ecological controls. The sediment was generally a net sink of NO_3^- and NH_4^+ in both sites, with several fold higher rates for NO_3^- uptake. MPB N demand could account for the entire sediment DIN uptake in Bonanza and 21% in Lebrija. The remaining high NO_3^- uptake rates indicate that they sustain elevated sediment denitrification rates. In contrast, rates of anaerobic oxidation of organic matter by Fe reduction and SO_4^{2-} reduction, estimated from Fe^{2+} and SO_4^{2-} vertical concentration profiles, were several orders of magnitude lower than the estimated water column-dependent denitrification rates. Overall, this study shows the importance of MPB in the Guadalquivir Estuary and the potential dominant role of denitrification in the anaerobic mineralization of organic matter.

KEYWORDS

Guadalquivir Estuary, hyperturbid estuary, seasonal variations, microphytobenthos, nutrients uptake, sediment-water column fluxes

1 Introduction

Coastal systems play a pivotal role in global biogeochemical cycles, buffering the exchange of matter and energy across terrestrial, oceanic, and atmospheric compartments. Among these systems, estuarine regions are renowned for their elevated productivity, driven by the influx of organic and inorganic matter from rivers and the autochthonous primary productivity of diverse organisms (Underwood and Kromkamp, 1999). The Guadalquivir Estuary, located in the Gulf of Cadiz (southwestern Spain), extends approximately 110 km from its mouth to the Alcalá del Río dam, Seville. It is one of the region's most ecologically and economically important estuaries, despite undergoing significant anthropogenic alterations since historical times. Such activities include urban and agricultural waste and recurrent dredging, which result in elevated turbidity and very high nutrient concentrations in the water column (Ruiz et al., 2017; Díez-Minguito and de Swart, 2020; Miró et al., 2022). Nitrate concentrations higher than 500 μM are frequently recorded at the head of Guadalquivir Estuary (Mendiguchía et al., 2007; Flecha et al., 2015). A high concentration of suspended particulate matter has been also frequently observed (>500 mg L^{-1}) reaching up to 30 g L^{-1} during an extreme turbidity event (Megina et al., 2023). This high turbidity affects various components of the biological community such as the macrofauna and small fishes (Donázar-Aramendía et al., 2019; Miró et al., 2020, 2022). In addition, the very high turbidity, which significantly reduces the photic layer, limits autochthonous phytoplankton primary production resulting in a net heterotrophic water column (Soetaert et al., 2006; Flecha et al., 2015; Ruiz et al., 2017; Huertas et al., 2018). However, the intertidal sediments in the Guadalquivir River banks are inhabited by a conspicuous benthic microalgal community known as microphytobenthos (MPB), which might contribute significantly to the autochthonous primary production within the estuary explaining part of its high productivity (Schutte et al., 2018; Donázar-Aramendía et al., 2019; Díez-Minguito and de Swart, 2020; Miró et al., 2020).

The MPB community, generally dominated by diatoms, includes cyanobacteria and other microalgal taxa (Underwood and Kromkamp, 1999). MPB plays a significant ecological and biogeochemical role in estuarine ecosystems in addition to their contribution to the total C fixation as primary producers (Underwood and Kromkamp, 1999; Sundbäck and Miles, 2002; Haro et al., 2019). MPB is an important food source both directly for marine meiofauna and macrofauna (Middelburg et al., 2000) and indirectly due to the production of exopolymers that serve as a carbon source for heterotrophic bacteria (Bohórquez et al., 2017). In addition, these exopolymers promote sediment cohesion and stabilization, and enhance water quality, as well (Paterson, 1989; Yallop et al., 1994). Furthermore, MPB plays a crucial role in the mineralization of organic matter and nutrient recycling by influencing sediment oxygen levels, organic matter lability, and the exchange of nutrients between the sediment and water column. The rate and pathways of organic matter mineralization, as well as the partitioning between aerobic and anaerobic metabolism, such as denitrification and sulfate and iron reduction, can be strongly influenced directly and indirectly by MPB activity due to oxygen production during daytime photosynthesis. Nitrogen demand by MPB can also affect coupled nitrification–denitrification in estuarine sediments and therefore nitrogen speciation and exchange rate across the sediment–water interface (Risgaard-Petersen, 2003; Soetaert et al., 2006; Schutte et al., 2018; Høgslund et al., 2023; Rios-Yunes et al., 2023).

Despite the evident presence of MPB in the Guadalquivir intertidal riverbanks, there is no information on its role as a potential contributor to total autochthonous primary production and biogeochemical cycling at the sediment–water interface in this important and very turbid temperate estuary. Therefore, the main objective of this study was to investigate the seasonal variations in MPB biomass and net metabolism, to analyze the spatiotemporal changes in nutrient concentrations, and to assess the fluxes of inorganic nutrients between the sediment and the water column. To the best of our knowledge, this is the first study that describes the main biogeochemical characteristics of the Guadalquivir Estuary intertidal sediments and evaluates the potential role of MPB, complementing the better-studied water column. These data contribute to obtaining a more integrated view of the biogeochemical and ecological characteristics of the system.

2 Material and methods

2.1 Study site and sampling

The Guadalquivir estuary (Figure 1), located in the southwest coast of the Iberian Peninsula, is approximately 110 km long and 150 m–800 m wide (Navarro et al., 2011). It is affected by a semidiurnal tidal cycle, with a maximum spring tidal range of 3.5 m (Díez-Minguito et al., 2012). The watershed is in a warm-temperate climate area with hot and dry summers and irregular rainfall characterized by oceanic storms. However, the river discharge is controlled by the net of dams in the watershed and ultimately by the Alcalá del Río dam (Supplementary Figure S1), located in the upper section (not shown in the map of Figure 1). Two sampling sites were selected along the estuary to cover a wide range of salinity: (i) Lebrija (36°57′27.9″N 6°10′36.7″W), with low-salinity range (from 1 to 7 PSU), and (ii) Bonanza (36°52′33.2″N 6° 20′58.2″W), near the mouth of the estuary, with higher salinity values (from 10 PSU to 23 PSU). At each sampling site, five sediment cores (5 cm Ø, 30 cm length) and *in situ* water (30 L) were collected on new moon quarterly (November 2018, February, May, August, and November 2019). Sediment samples were collected in the bare muddy intertidal zone along the riverbanks during emersion. Samples were collected from an area of approximately 2 m^2 in each site, avoiding fragments of vegetation or leaves in the collected samples in a time range of ±50 min from low tide. Tidal amplitudes throughout the sampling period did not change in Bonanza (~1.1 m), whereas those in Lebrija were 1.1 m in November 2018, 0.8 m in February and November, and 1 m in May and August 2019. Water samples were collected as close as possible to the sediment cores (a few meters). Sediment cores and *in situ* water were immediately transported to the laboratory, where the cores were placed in two 12-L aquaria (one for Bonanza and the

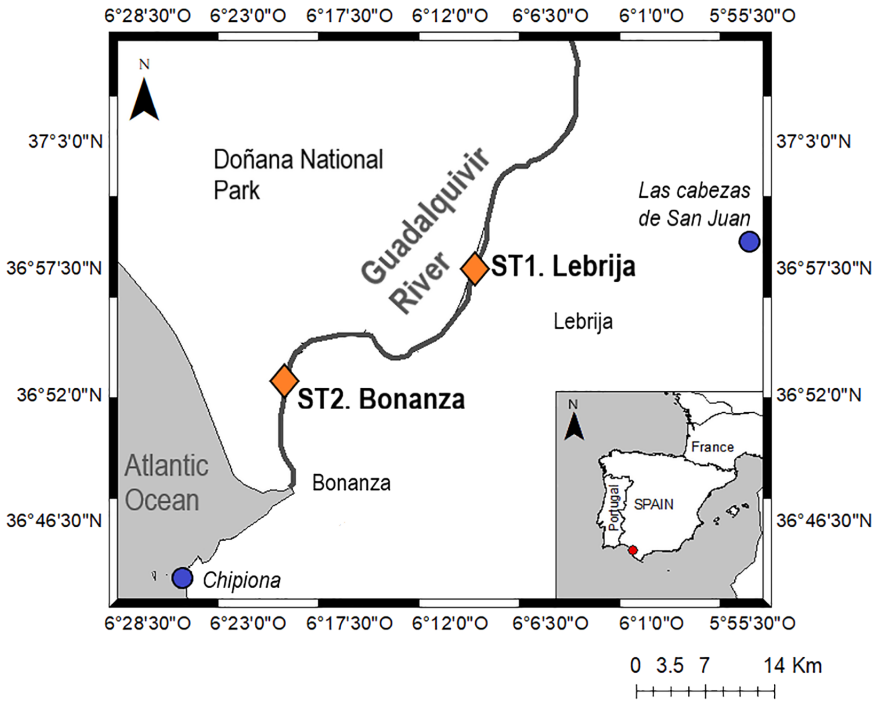

FIGURE 1
Map of the lower Guadalquivir estuary indicating the location of the two sampling sites (orange rhombs). The locations of the closest weather stations (blue dots) are also shown.

other for Lebrija) filled with *in situ* water and maintained in a temperature-controlled room at 18°C. Sediment cores were illuminated with white LED lamps (Lince 6M Verso, Light Environment Control S. L.) at an irradiance of 1,300 µmol photons m^{-2} s^{-1} measured at the water interface.

2.2 Total suspended solids and inorganic nutrients in the water column

Monthly samplings of some water column variables were done at new moon at the same sampling sites, Lebrija and Bonanza, from a boat with a multiparameter probe (EXO2, YSI), anchored at approximately 10 m from the shore and at the same time range from low tide (data in Table 1). Surface water samples were taken for the measurement of total suspended solids (TSS) and inorganic nutrients during the sediment sampling period, from November 2018 to November 2019. For TSS, the water samples were filtered over preweighed GF/F filters and weighed again after drying at 60°C. The filtered water was collected for the measurement of inorganic nutrients. In addition, coinciding with the sediment sampling dates (every 3 months), water column samples were collected to measure only inorganic nitrogen species, close to the sediment core sampling sites. All water samples were immediately filtered through a GF/G filter and stored frozen (−20°C) until analysis. Inorganic nitrogen nutrient concentrations were measured spectrophotometrically on a microplate reader (Multiskan GO, Thermo Scientific), following methods described by Bower and Holm-Hansen (1980) for NH_4^+ and García-Robledo et al. (2014) for NO_3^- and NO_2^-. PO_4^{3-} and SiO_4^{4-} were determined following Grasshoff et al. (1999).

2.3 Sediment–water fluxes of oxygen and inorganic nitrogen

Sediment–water fluxes were measured the day after sampling by whole-core incubations in light and dark conditions. Light and dark incubations were performed sequentially in the same sediment cores after a minimum of 1 h of preincubation at the same light condition. For the incubations, sediment cores (n = 5, circa 20 cm of sediment and 10 cm of water column) were closed with transparent Plexiglas lids and kept closed for 2 h–7 h depending on season. The

TABLE 1 Monthly averages ± SD of temperature (°C), salinity (PSU), total suspended solids (TSS, mg L^{-1}) and inorganic nutrients (DIN = NO_3^- + NO_2^- + NH_4^+, PO_4^{3-}, and SiO_4^{4-}, µmol L^{-1}) in the water column at low tide, from November 2018 to November 2019 (n = 14), in Bonanza and Lebrija, in the Guadalquivir estuary.

	T	Salinity	TSS	DIN	PO_4^{3-}	SiO_4^{4-}
Lebrija	19.5 ± 5.3	5.3 ± 3.1	325.4 ± 188.7	341.6 ± 148.2	2.9 ± 0.9	81.4 ± 137.4
Bonanza	19.2 ± 5.2	15.9 ± 6.0	91.8 ± 63.0	246.0 ± 111.5	2.4 ± 0.9	59.1 ± 105.8

duration of incubations was adjusted to avoid oxygen variations of more than 20%.

Inorganic nitrogen (NH_4^+, NO_3^-, NO_2^-) concentrations were measured in water samples collected in the water column of the cores before and after the incubations. All water samples were immediately filtered through a GF/G filter and stored frozen (−20°C) until analysis as already described. Sediment–water fluxes (J, mmol m^{-2} h^{-1}) of inorganic nitrogen species were calculated as the difference between the initial and final concentrations during the incubation according to the following equation (Equation 1):

$$J = \frac{(C_{final} - C_{initial})}{\Delta t} \times \frac{V}{A} \quad (1)$$

where C is the concentration of the solute (mmol/m^3), V represents the volume of the water column in the core (m^3), A represents the area of the sediment core (m^2), and Δt is the incubation time interval (hours). Positive and negative fluxes represent nutrient efflux from the sediment and sediment net uptake, respectively.

To measure O_2 fluxes, changes in O_2 concentration during the incubations were measured every 30 s in each core by using optical oxygen sensors (OXSP5, PyroScience®). Oxygen fluxes at the sediment water interface (net community production, NCP, fluxes measured in light conditions; and dark respiration, R_{dark}, fluxes measured in dark conditions) expressed by unit of surface (mmol O_2 m^{-2} h^{-1}) were calculated as the slope of the changes in oxygen concentration with time (mmol O_2 m^{-3} h^{-1}) and normalized to the area and volume of the water column during the incubation similarly to Equation 1, except that $\Delta[O_2]/\Delta t$, was obtained from the slope of continuous changes in O_2 concentration over time.

Daily net community production (DNCP) was calculated from NCP and R_{dark}, taking into account the seasonal changes in the local daylight (t_L) and night (t_D) periods, according to DNCP = $NCP \times t_L - R_D \times t_D$.

2.4 Inorganic nitrogen, iron, sulfate, and dissolved inorganic carbon in the porewater

Once the incubations were completed, the five sediment cores were sliced into 1-cm-thick slices down to the 10-cm depth. The sediment was centrifuged at 4,700 ×g for 20 min at 4°C to extract the porewater. The sediment pellet was freeze-dried and preserved in darkness for further analyses (chlorophyll, organic carbon and total nitrogen, see following section).

For inorganic nitrogen (NH_4^+, NO_3^-, and NO_2^-), porewater samples collected were preserved and analyzed as described above for the water column. For Fe^{2+} analysis, 0.4 mL of porewater was transferred to Eppendorf tubes with 0.1 mL of HCl 2N to avoid oxidation. Fe^{2+} was measured following Viollier et al.'s method (Viollier et al., 2000). Sulfate (SO_4^{2-}) was analyzed by ion chromatography in aqueous matrices (METROHM:858-Professional Sample processor) (INMAR Peripheral Services).

For dissolved inorganic carbon (DIC) analysis, 1 mL of porewater was transferred to 3-mL Exetainers (Labco, UK) with 2 mL of MQ water and preserved with 0.1 mL of 37% formalin. DIC in the porewater was determined by a colorimetric method (Sarazin et al., 1999). Calibration was performed with standards spiked with the same amount of formalin than the samples.

Production/consumption rates of NH_4^+, Fe^{2+}, SO_4^{2-}, and DIC were calculated from their concentration profiles within the sediment using the software PROFILE (Berg et al., 1998). The porosity used in calculation was an average of the porosity measured in the samples (0.75). Irrigation and bio-diffusivity was considered as negligible. The diffusion coefficients were extracted from Li and Gregory (1974).

2.5 Organic matter, organic carbon, total nitrogen, and chlorophyll in the sediment

Organic carbon (C_{org}) was determined as the difference between the total carbon measured in the freeze-dried sediment samples and inorganic carbon measured on a replicate previously combusted at 550°C for 4 h. Total nitrogen was measured in the freeze-dried sediment samples. Both samples were analyzed on an elemental analyzer (Leco CHNS 932) at the Central Services of the University of A Coruña, Spain.

Photosynthetic pigments were extracted from freeze-dried sediment (circa 1.5 g) in 100% methanol buffered with $MgCO_3$. After 18 h in darkness at 4°C, absorbance spectra of the extracts were measured on a microplate reader (Multiskan GO; Thermo Scientific) before and after acidifying with 100 µL of 1 N HCl. Chlorophyll *a* (Chla) and phaeophytin *a* (Phaeoa) were measured according to Stal et al. (1984). Active chlorophyll was estimated as the ratio between Chla and Phaeoa (Chla/Phaeoa) in each sample.

2.6 Statistical analysis

In order to explore statistical differences in our data, variables were first graphically checked for extreme values or skewed distributions (Zuur et al., 2010). Sediment Fe^{2+}, NO_3^-, NO_2^-, Chla, and Phaeoa were ln(x+1) transformed. Analysis was performed on each variable individually by PERMANOVA in PRIMER 6.0 (PRIMER-e Ltd) using a Euclidean distance similarity index and 1,000 permutations. When permutations were low, a Monte Carlo approximation was used to obtain the p values (Anderson et al., 2008). *Post-hoc* tests were performed when a significant effect was found. If a significant interaction was observed, *post-hoc* tests were performed within the other factor.

Differences in water column concentrations were tested for the effects of time and location. Sediment-water fluxes were analyzed separately for light and in darkness with time and location and their interaction as fixed factors. In order to test whether a difference existed in the magnitude of nutrient fluxes between light and darkness, an analysis was performed using the paired difference for each core between light and dark incubation. For the sediment column variables, i.e., solid phase and porewater solutes, time, location, and depth were tested as fixed factors. Since depth intervals within cores are not independent, core identity was

introduced as a random factor nested within site and time. The interactions of time by location, and depth by location, were also included in the model. Correlations between variables were tested with a Spearman rank correlation coefficient.

Statistical significance was established at $p<0.05$. All the results were expressed as mean ± SE unless otherwise stated. All results are interpreted through the "lens of statistical clarity" sensu Dushoff et al., 2019.

3 Results

3.1 Organic carbon and total nitrogen content in the sediment

The organic carbon content in the sediment (C_{org}) in both sites showed a slight trend to decrease with depth (Figure 2A) ($p <0.0001$; Supplementary Table S2). C_{org} was generally higher in Bonanza (5.29 mg cm^{-3}–11.72 mg cm^{-3}) than in Lebrija (4.93 mg cm^{-3}–8.85 mg cm^{-3}) (Supplementary Figure S2; Figure 2A), although the difference was statistically clear only in July and November 2019 (post-hoc test, $p < 0.05$; Supplementary Table S5). C_{org} changed along the year within each site with differences being clear in some of the months (*post-hoc*, $p < 0.05$; Supplementary Table S5), but seasonal changes were not synchronous in both sites (Figure 2A).

Total nitrogen (N_T) content range was similar in Bonanza and Lebrija (0.35 mg cm^{-3}–0.91 mg cm^{-3} and 0.31 mg cm^{-3}–0.75 mg cm^{-3}, respectively), although statistically clear interactions were observed between site and depth and site and date ($p < 0.0001$; Supplementary Table S2). At both sites, values showed differences with sediment depth (*post-hoc*, $p <0.05$; Supplementary Table S5) with highest values observed near the surface (Supplementary Figure S2B; Figure 2B). N_T showed clear differences with time in both sites. N_T showed clearly lowest values in November 2018 and February in Bonanza, whereas in Lebrija statistically clearly higher values were observed in February compared with the rest of months (Figure 2B) (*post-hoc*, $p <0.045$; Supplementary Table S5).

The molar ratio of C_{org} to N_T (C:N) (Supplementary Figure S2C) was usually higher in Bonanza than in Lebrija, although only in August and November 2019 was this difference statistically clear (*post-hoc*, $p < 0.026$; Supplementary Table S5). The mean C:N ratio measured in Bonanza was 15.48 ± 0.98 mol/mol and 12.25 ± 0.35 mol/mol in Lebrija.

3.2 Photosynthetic pigments content in the sediment

Chla concentrations in the sediment were highest at the sediment surface, decreasing exponentially with depth (Figure 2C; Supplementary Figure S2D) (*post-hoc*, $p < 0.05$; Supplementary Table S5). The annual mean Chla concentration in the upper 1-cm sediment layer was higher in Bonanza than in Lebrija, being 11.48 ± 1.45 μg cm^{-3} and 8.48 ± 0.94 μg cm^{-3}, respectively. Chla showed clear differences with season at both sites (*post-hoc*, $p < 0.05$; Supplementary Table S5). The highest concentrations were measured in February and November 2019, reaching up to 13.00 ± 2.73 μg cm^{-3} and 20.25 ± 2.16 μg cm^{-3} in Bonanza and 14.16 ± 3.85 μg cm^{-3} and 9.33 ± 0.26 μg cm^{-3} in Lebrija, respectively. The lowest values were found in August, being 6.44 ± 1.62 μg cm^{-3} and 5.40 ± 0.70 μg cm^{-3} in Bonanza and Lebrija, respectively.

The ratio between Chla and Phaeoa (Chla : Phaeoa) was not clearly different between Bonanza (range from 0.01 ± 0.02 to 0.67 ± 0.09) and Lebrija (from 0.03 ± 0.01 to 0.47 ± 0.20), although a significant interaction was found ($p < 0.001$; Supplementary Table S2). The seasonal changes of Chla : Phaeoa followed a similar spatiotemporal evolution to that of Chla, with some exceptions. In Bonanza, the highest values of Chla : Phaeoa were observed at August at the sediment surface, whereas in Lebrija, this occurred in November at the deepest sediment layer (Figure 2D).

3.3 Oxygen fluxes at the sediment–water interface

The microbenthic community from both sampling sites were photosynthetically active in light conditions (Figure 3A). Net community production during light (NCP) was clearly higher in Bonanza than Lebrija (*post-hoc*, $p < 0.019$; Supplementary Table S5), with the exception of February, with mean values of 5.42 ± 3.58 mmol m^{-2} h^{-1} and 1.54 ± 2.24 mmol m^{-2} h^{-1}, respectively (Figure 3A). Respiration rates in darkness (R_{dark}) were 2.38 ± 0.14 mmol m^{-2} h^{-1} in Bonanza, being on average 1.8 times higher than those measured in Lebrija (1.31 ± 0.49 mmol m^{-2} h^{-1}) (Figure 3B). Highest values of NCP were observed in August in Bonanza (*post-hoc*, $p < 0.003$; Supplementary Table S5), and in February in Lebrija (*post-hoc*, $p < 0.001$; Supplementary Table S5). R_{dark} covaried in both sampling sites along the seasonal cycle and was highest in May, followed by August. Differences between months were clearly higher in Bonanza than Lebrija. In both Bonanza, DNCP was always positive ranging from 21.4 m^{-2} day^{-1} to 129.8 mmol O_2 m^{-2} day^{-1} in November 2019 and August, respectively. In Lebrija, it ranged from –23.3 mmol O_2 m^{-2} day^{-1} to 43.9 mmol O_2 m^{-2} day^{-1}, showing positives values only in February and August.

3.4 Inorganic nutrients in the water column and sediment porewater

Dissolved inorganic nitrogen (DIN) was the dominant nutrient in the Guadalquivir water column in Bonanza and Lebrija during the studied period (Table 1). The most abundant inorganic nitrogen nutrient in the water of Guadalquivir River was nitrate (90%–99.7% of DIN). Nitrate concentrations in the water column showed statistically clear seasonal changes between all months in Lebrija and the majority in Bonanza (*post-hoc*, p-value <0.039; Supplementary Table S5) (Figure 4A). Seasonal maximum nitrate concentration was found in February 2019 with values up to 395 μM and 639 μM in Bonanza and Lebrija, respectively. The minimum nitrate concentration was measured in August (30 μM–40 μM), 10 times lower than the maximum measured in February. Concentrations increased again in November 2019 up to 93 μM and 257 μM in Bonanza and Lebrija, respectively (Figure 4A). Nitrite concentrations were close to detection

10.3389/fmars.2024.1389673

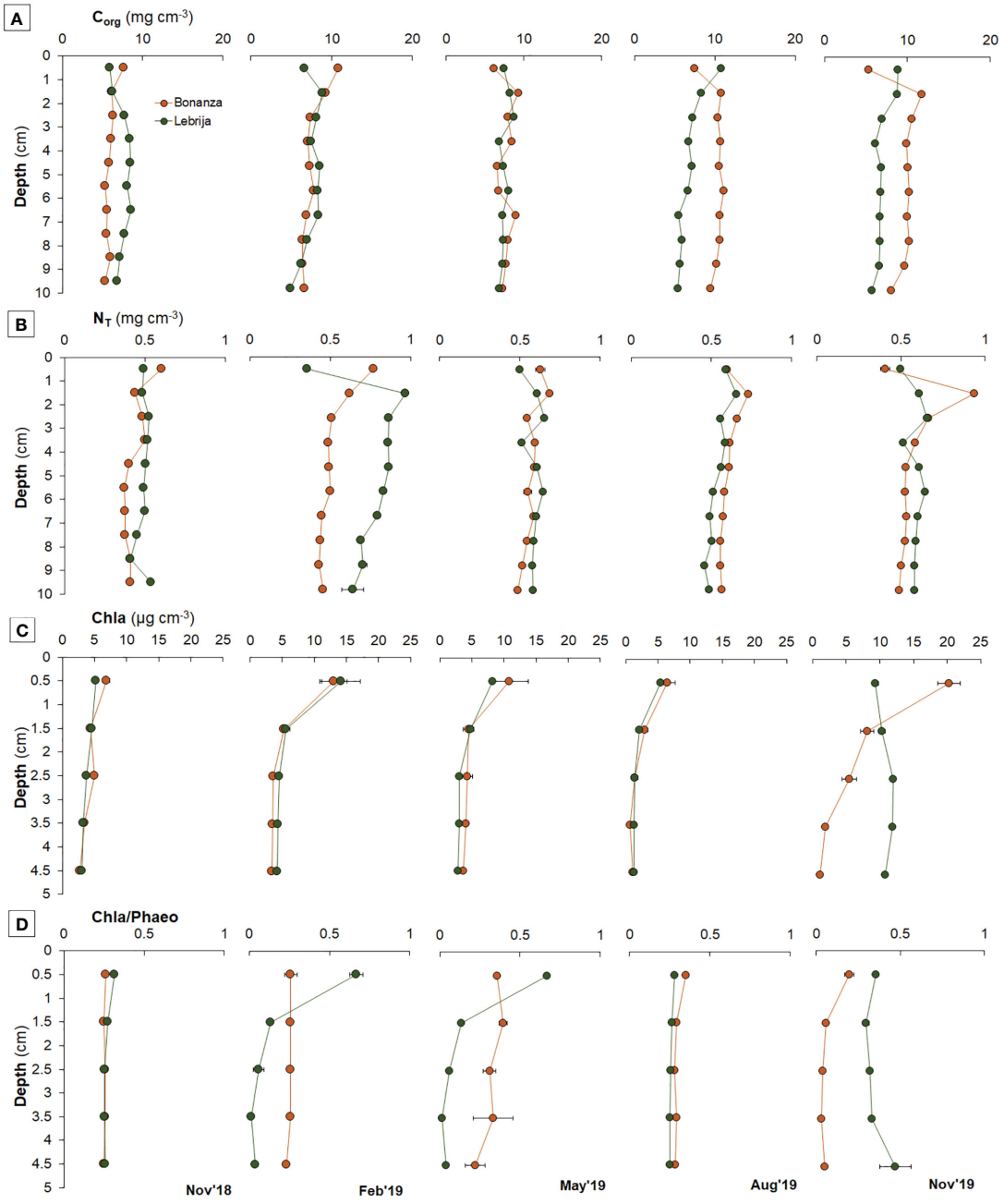

FIGURE 2
Seasonal changes in sediment **(A)** organic carbon (C_{Org}), **(B)** total nitrogen (N_T), **(C)** chlorophyll-a (Chla) contents, and **(D)** in Chlorophyll-a: Phaeophytin-a ratio in the first 10 cm in Bonanza (orange dots and lines) and Lebrija (green dots and lines) along the Guadalquivir estuary, from November 2018 to November 2019. Data points represent means ± SE (n = 3).

limits never exceeding 2 µM (Figure 4B). The ammonium concentration in the water column ranged from 0.15 µM to 10.7 µM, with two peaks in May and November 2019 (Figure 4C). Water column ammonium was similar in both sampling sites except in February and May, when higher concentrations were measured in Bonanza, but these were not statistically clear ($p > 0.05$, Supplementary Table S5). PO_4^{3-} concentrations were approximately 2 µM–3 µM in both sites, the N:P stoichiometric ratio was much higher than the typical one for phytoplankton (16). The mean dissolved SiO_4^{4-} concentration was 81.4 ± 137.4 and 59.1 ± 105.8 (mean ± SD), in Lebrija and Bonanza, respectively, but dropped to 26.2 ± 7.8 µM and 16.7 ± 6.9 µM when the very high concentrations (up to 474.5 µM and 362.9 µM measured in November and December 2018, respectively) were excluded from annual averages (Table 1).

Porewater NH_4^+ levels greatly exceeded those in the water column, increasing significantly with depth at both stations. Concentrations ranged from 2 µM–35 µM in the top centimeter to maximum values of 390 µM–490 µM at 10-cm depth. Differences were statistically clear

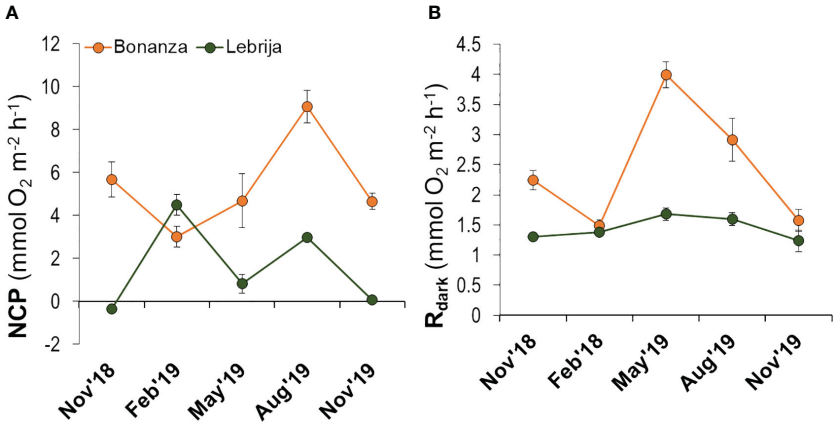

FIGURE 3
Seasonal changes in **(A)** net community production in light and **(B)** dark respiration estimated from the O_2 fluxes across the sediment-water column interface in Bonanza (orange) and Lebrija (green) along the Guadalquivir estuary during the sampling period, from November 2018 to November 2019. Data points represent means ± SE (n = 5).

down to 4.5 cm in Lebrija, whereas in Bonanza they were even deeper (*post-hoc*, $p < 0.019$; Supplementary Table S5) (Supplementary Figure S2; Figure 5A). Clear seasonal differences were observed mainly within February compared with the rest of the months in Lebrija and February and November 2019 for Bonanza (*post-hoc*, $p < 0.05$; Supplementary Table S5). While high values were recorded with depth in both sites in August, in February concentrations were high in Bonanza but low in Lebrija (Figure 5A). Porewater NO_3^- and NO_2^- were detected in the top 2 cm of sediment, rapidly decreasing with depth (Supplementary Figure S2; Figure 5). Concentrations of NO_3^- and NO_2^- in the sediment varied over time, with different patterns at each station. However, the lowest concentrations were observed at both sites in August (Figures 5B, C).

3.5 Dissolved inorganic carbon, iron, and sulfate in the sediment porewater

The concentrations of dissolved inorganic carbon in the sediment (DIC) showed a similar range in Bonanza and Lebrija (4.47 mM–12.10 mM and 2.29 mM–11.97 mM, respectively) but was clearly different between sites (*post-hoc*, $p < 0.016$; Supplementary Table S5) with the exception of February and August. In both sites, DIC increased with depth (Supplementary Figure S2K; Figure 6A) with the exception of the bottom samples in Bonanza (*post-hoc*, $p < 0.001$; Supplementary Table S5). In addition, for most dates average values with depth DIC varied throughout the year at both sites although out of phase (*post-hoc*, $p < 0.05$; Supplementary Table S5) (Figure 6A).

Porewater Fe^{2+} concentrations ranged from 0.05 µM to 416 µM in Lebrija and up to 826 µM in Bonanza (Figure 6B), showing clear differences between sites with the exception of August (*post-hoc*, $p < 0.05$; Supplementary Table S5). The Fe^{2+} profiles observed at both Lebrija and Bonanza remained relatively stable throughout the year, showing consistent and similar initial concentrations down to a depth of approximately 2.5 cm where the iron concentration gradually increased for a few centimeters before decreasing again. For both sites, the highest average Fe^{2+} concentration was recorded in August, with Bonanza twice as high as Lebrija. Differences between depths were more clear in Bonanza than in Lebrija (*post-hoc*, $p < 0.05$; Supplementary Table S5).

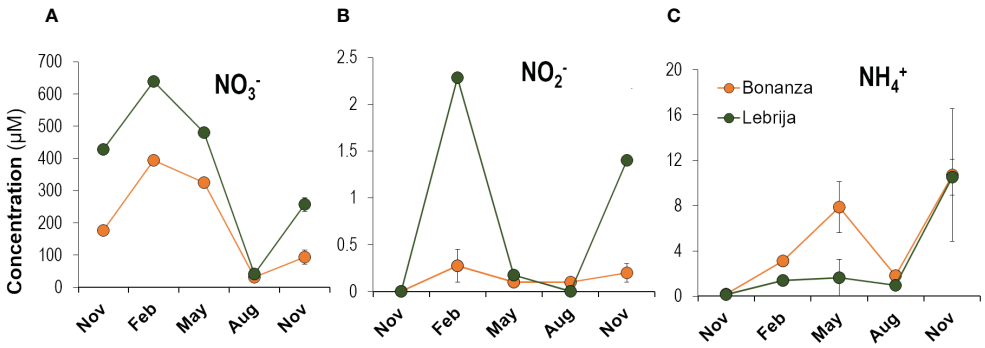

FIGURE 4
Seasonal changes in **(A)** NO_3^-, **(B)** NO_2^-, and **(C)** NH_4^+ concentrations in the water column in Bonanza and Lebrija along the Guadalquivir estuary during the sampling period, from November 2018 to November 2019. Data points represent means ± SE (n = 3).

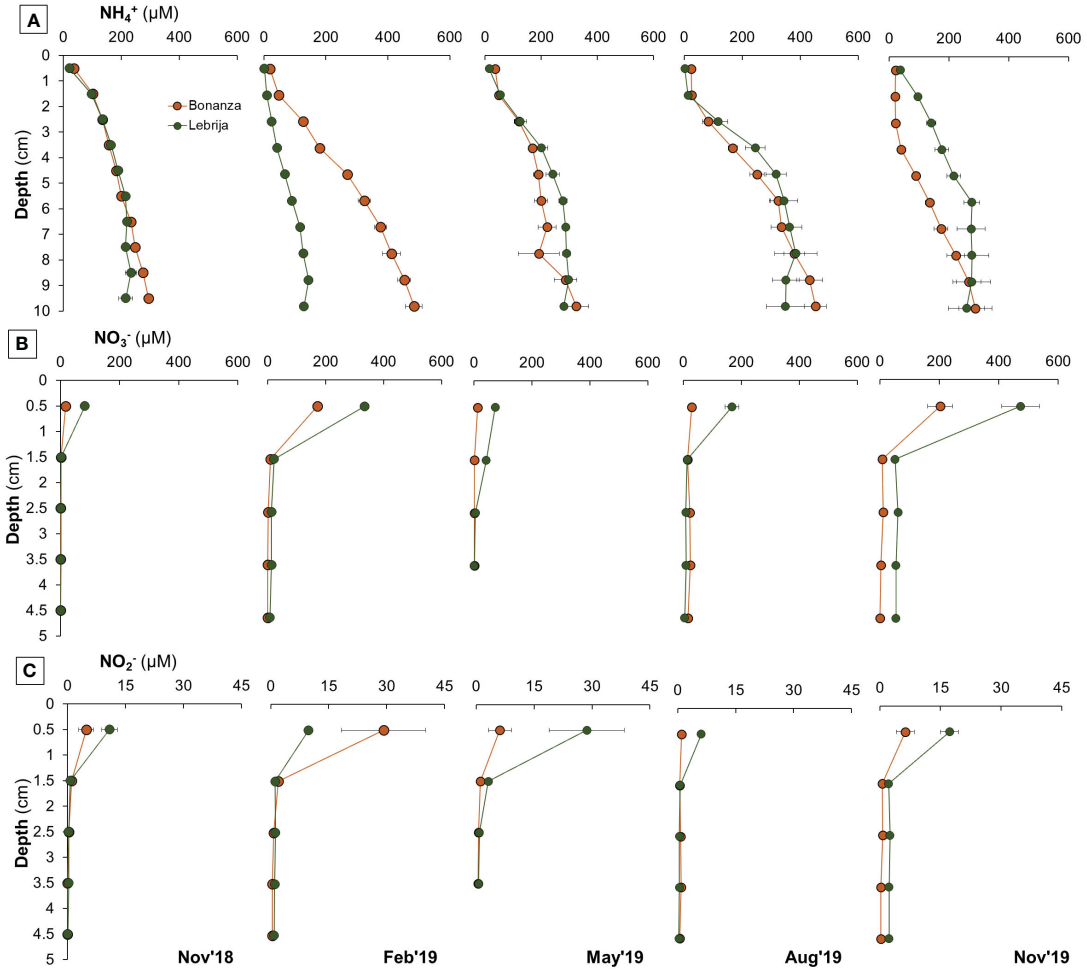

FIGURE 5
Seasonal changes in sediment porewater concentrations of **(A)** ammonium (NH_4^+), **(B)** nitrate (NO_3^-), and **(C)** nitrite (NO_2^-) in the first 10 cm in Bonanza (orange dots and lines) and Lebrija (green dots and lines) along the Guadalquivir estuary during the sampling period, from November 2018 to November 2019. Data points represent means ± SE (n = 3).

SO_4^{2-} porewater content ranged from 9.23 ± 1.27 mM to 11.85 ± 1.72 mM at Bonanza and between 4.40 ± 0.50 mM and 5.48 ± 0.54 mM at Lebrija, showing statistically clear differences between the two sampling sites ($p < 0.001$) (Figure 6C).

3.6 Fluxes of inorganic nitrogen at the sediment-water interphase

Net NH_4^+ fluxes across the sediment–water interface measured by whole core incubations were generally negative throughout the measured period (–0.96 mmol m^{-2} $h^{-1}$to 0.32 mmol m^{-2} h^{-1}), indicating net consumption rates by the sediment at both locations (Figure 7A). NH_4^+ fluxes in Lebrija were generally lower than in Bonanza with no changes in the direction or magnitude between light and dark fluxes ($p > 0.05$). In contrast, in Bonanza, differences between light and dark fluxes were statistically clear (*post-hoc*, $p < 0.05$; Supplementary Table S5) with the exception of February.

Net NO_3^- fluxes (from −2.55 ± 1.55 mmol m^{-2} h^{-1} to 2.03 ± 1.63 mmol m^{-2} h^{-1}) followed a similar seasonal trend in both sites and were approximately one order of magnitude higher than those of ammonium (Figure 7B). NO_3^- fluxes, both in light and in darkness, were negative during November 2018 and February 2019, suggesting a nitrate uptake by the sediment, decreasing in May and August to values around zero. This difference was clear in darkness for both sites (*post-hoc*, $p < 0.05$; Supplementary Table S5) whereas in light differences over time were found only in Lebrija. In November 2019, there was a considerable scattering in the measured nitrate fluxes, both in absolute values and in the direction across the sediment–water interface.

Net NO_2^- fluxes (from −0.03 mmol m^{-2} h^{-1} to 0.10 mmol m^{-2} h^{-1}) were lower than ammonium and nitrate fluxes. Net NO_2^- fluxes showed a peak of efflux in May showing statistically clear interactions with season and site ($p < 0.0001$; Supplementary Table S3) (Figure 7C).

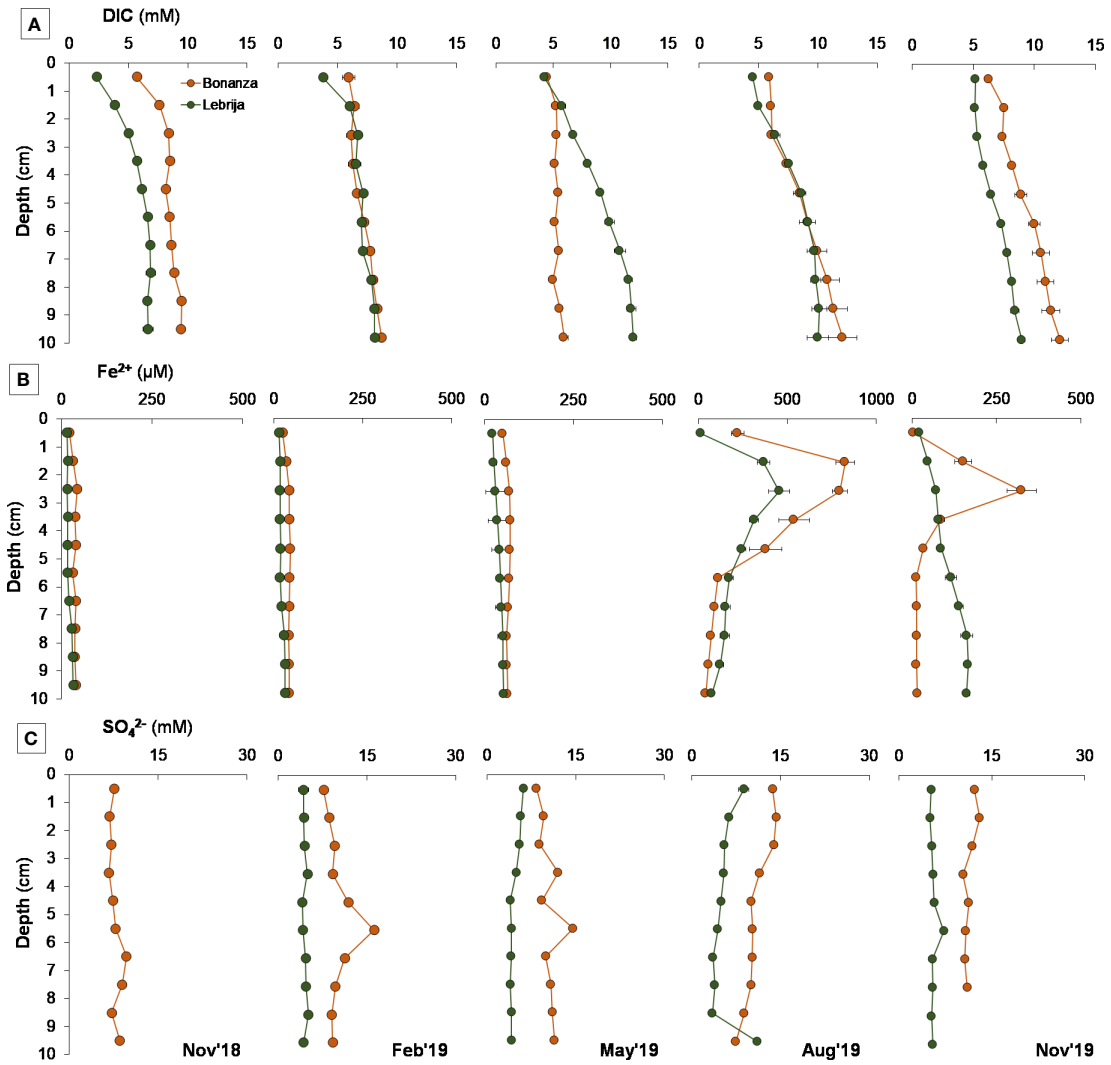

FIGURE 6
Seasonal changes in sediment porewater concentrations of **(A)** DIC, **(B)** Fe^{2+}, and **(C)** SO_4^{2-} in the first 10 cm in Bonanza (orange dots and lines) and Lebrija (green dots and lines) of the Guadalquivir estuary during the sampling period, from November 2018 to November 2019. Data points represent means ± SE (n = 3). November 2018 samples for SO_4^{2-} in Lebrija were lost (white area).

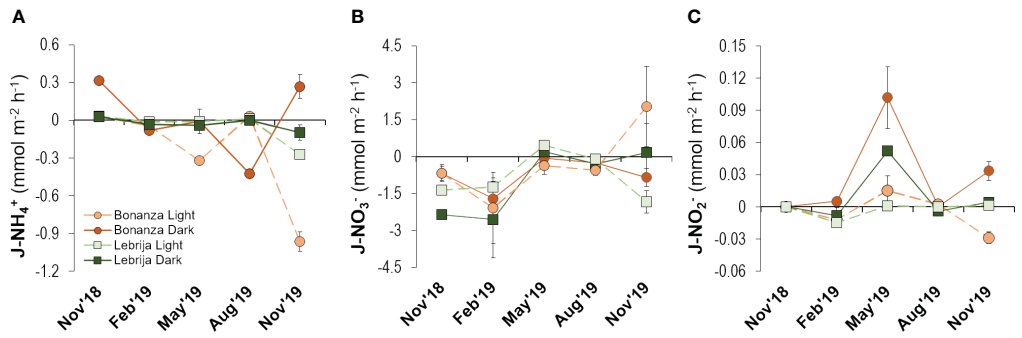

FIGURE 7
Seasonal changes in **(A)** NH_4^+, **(B)** NO_3^-, and **(C)** NO_2^- fluxes in light and in darkness across the sediment–water column interface in Bonanza (orange) and Lebrija (green) along the Guadalquivir estuary during the sampling period, from November 2018 to November 2019. Data points represent means ± SE (n = 5).

3.7 Net production rates of DIC, NH_4^+, and Fe^{2+} and net consumption rate of SO_4^{2-} within the sediment

Net production (DIC, NH_4^+, and Fe^{2+}) and consumption rates (SO_4^{2-}) in the sediment were calculated modeling the porewater profiles (Figures 5, 6) with the PROFILE software (Berg et al., 1998). Net DIC production within the sediment ranged from 0.30 ± 0.05 mmol m^{-2} h^{-1} to 1.29 ± 0.14 to mmol m^{-2} h^{-1} in Bonanza and from 0.36 ± 0.09 mmol m^{-2} h^{-1} to 0.94 ± 0.47 mmol m^{-2} h^{-1} in Lebrija (Supplementary Figure S3A). Two relative maxima were found in Bonanza in May and November 2019, whereas in Lebrija they were found in February and August 2019. Net NH_4^+ production rates in Bonanza ranged from 3.17 µmol m^{-2} h^{-1} in May and November 2019 to 19.37 µmol m^{-2} h^{-1} in November 2018 (Supplementary Figure S3B). In Lebrija, two NH_4^+ production rates maxima were found in November 2018 and August 2019 with values up to 35.70 µmol m^{-2} h^{-1} and minimum values of 18.69 µmol m^{-2} h^{-1} in February 2019. Net production of NO_3^- and NO_2^- could not be estimated using PROFILE because both nutrients were restricted to the upper cm of sediment (Figure 5).

Net Fe^{2+} production rate represents an estimation of iron reduction microbial pathway within the sediment. Fe^{2+} production rates showed very low values between November 2018 to May 2019, increasing in August 2019 up to values of 164.93 µmol m^{-2} h^{-1} and 69.12 µmol m^{-2} h^{-1} at Bonanza and Lebrija, respectively (Supplementary Figure S3C). Net SO_4^{2-} consumption rates allow us to estimate sulfate reduction activity within the sediment. These rates showed values between −15.48 µmol m^{-2} h^{-1} and 17.43 µmol m^{-2} h^{-1}, with maximum values in May and November 2019 at Bonanza and Lebrija, respectively (Supplementary Figure S3D).

4 Discussion

4.1 Organic carbon and total nitrogen

The concentrations of organic carbon (C_{org}) and total nitrogen (N_T) in intertidal sediments of the Guadalquivir Estuary were lower than in the nearby intertidal sediments of Cadiz Bay (Corzo et al., 2009; Bohórquez et al., 2019; Haro et al., 2020), but similar to those observed in its sublittoral sediments (Burgos et al., 2018a) and in other temperate estuaries (Rios-Yunes et al., 2023). The relatively scarce differences in the vertical distribution of C_{org}, N_T, and C:N with depth (Supplementary Figure S2) indicated that sediments are well mixed in the upper 10-cm depth (Canfield et al., 2005). Bonanza exhibits clearly higher C_{org} in some months but similar NT to Lebrija, resulting in higher C:N ratios at the more marine site (Figure 2, Supplementary Figure S2). Despite this difference among sites, C:N ratios in the Guadalquivir Estuary were similar to other muddy intertidal environments (Cabrita and Brotas, 2000; Haro et al., 2020; Rios-Yunes et al., 2023). C:N ratio >10 in the sediment surface suggests that, in addition to autochthonous production by MPB or phytoplankton, there is a certain contribution of allochthonous organic matter from the river catchment area (Hedges et al., 1997; Hillebrand and Sommer, 1999). Seasonal differences in C_{org} and N_T were statistically clear in both sites, although they depended on the site, with peaks in November. This seasonal pattern coincided with seasonal changes in Chl *a*, as discussed in the following section. Nonetheless, it was likely affected as well by seasonal changes in the annual precipitation pattern and the management of river flow in the Alcala de Rio dam (Supplementary Figure S1). Precipitation was high in February and November and might have increased the contribution of allochthonous organic matter to the sediment.

4.2 Microphytobenthic biomass seasonal dynamics

Microphytobenthos biomass estimated by the Chla concentration decreased exponentially with depth within the sediment as expected (Supplementary Figure S2) (Macintyre et al., 1996; García-Robledo et al., 2010; Garcia-Robledo et al., 2016), except in Lebrija in November 2019, when the Chla concentration was similar down to 5-cm depth (Figure 2). This unusual sediment Chla vertical profile could be related to a higher sediment accumulation and resuspension following an opening of the Alcalá del Río dam (Supplementary Figures S1, S2) (Díez-Minguito et al., 2012). Chla followed a seasonal cycle with highest surface values in winter (February) and in fall (November) and a minimum in summer (August) in both sampling sites. The MPB biomass seasonal pattern in the Guadalquivir Estuary coincides with the MPB seasonal cycles recorded in the inner Bay of Cadiz (Garcia-Robledo et al., 2016; Haro et al., 2020, 2022). Furthermore, the Chla concentration range (3.76 µg cm^{-3}–13.50 µg cm^{-3}) was similar to that found in the Bay of Cádiz (Garcia-Robledo et al., 2016; Haro et al., 2020) and other estuarine zones around the world (Cabrita and Brotas, 2000; McTigue et al., 2015; Kwon et al., 2020). The higher values in November of 2019, not observed in 2018, are probably related to changes in the rainfall pattern, with more prolonged but lower-intensity rains, providing nutrients to the sediment surface. In fact, among the environmental variables studied, MPB biomass estimated by Chla was only positively correlated with water column NO_3^- ($r = 0.76$, $p < 0.05$, $n = 9$).

The Chla : Phaeoa ratio can be used as a proxy of the active chlorophyll since phaeopigments form in the water column and sediments due to microbial degradation and grazing (Lee et al., 2000; McTigue et al., 2015). The Chla : Phaeoa ratio in the Guadalquivir Estuary was usually <1, although in the surface layers in Bonanza, the ratio was slightly higher than in Lebrija (Supplementary Figure S2; Figure 2). The maximum of Chla : Phaeoa observed in summer in Bonanza at the sediment surface could be due to the higher grazing rate on MPB and microbial degradation rates during summer (Lee et al., 2000; McTigue et al., 2015). However, no such summer maximum was observed in the more riverine sampling point (Figure 2). In the intertidal sediments of the Guadalquivir River, the Chla and Phaeoa concentrations were statistically correlated with N_T content ($r = 0.52$ and 0.24, respectively, $p < 0.05$, $n = 150$), whereas the correlation with C_{org} was weaker for Chla ($r = 0.21$, $p = 0.01$, $n = 150$) not significant for

Phaeoa (r = 0.12, p = 0.16) Therefore, MPB biomass seems to contribute significantly to the pool of labile organic matter within the sediment, which usually has a higher N content and a higher turnover time.

4.3 Net metabolism in the Guadalquivir intertidal sediments

Net community primary production in light and respiration rate in darkness measured in this study have to be considered potential rates since they were measured at saturating light conditions or in the dark, respectively, and at constant temperature. These data are the first available on the benthic metabolism of intertidal sediments in the Guadalquivir Estuary. The sediment surface in the area is characterized by a macroscopically evident MPB biofilm dominated by diatoms. In general, NCP and R_{dark} were higher in Bonanza than in Lebrija, with values being similar to those measured in the Cadiz Bay (Burgos et al., 2018b; Haro et al., 2020) and other temperate estuarine intertidal sediments (Macintyre et al., 1996; Underwood and Kromkamp, 1999; Kwon et al., 2020). One notable contrast between the sites studied was the existence of very low or even negative NCP values in Lebrija, whereas Bonanza showed positive NCP throughout the year. This contrast was even more evident comparing their DNCP; the intertidal sediment community was always net autotrophic in Bonanza and could thus contribute positively to the overall primary production of the estuary along the year, whereas in Lebrija, positive values of DNCP were only observed in February and August.

The seasonal dynamics of NCP was different in Lebrija and Bonanza; however, R_{dark} followed the same pattern (Figure 3). We only observed an NCP annual maximum in Bonanza in August, whereas in Lebrija in addition to the peak in August, the annual maximum occurred in February. The spatiotemporal changes in net community production and respiration did not correlate clearly with any of the environmental variables measured in this study. Seasonal trends in NCP and R_{dark} did not coincide with changes in MPB standing stocks in the Guadalquivir Estuary (Figure 2). This lack of seasonal coupling was also observed in the sediments of the inner Bay of Cádiz, where the seasonal maximum in MPB biomass occurs in winter whereas MPB primary production peaks in summer (Garcia-Robledo et al., 2016; Haro et al., 2020). The absence of covariation between seasonal changes in MPB biomass and photosynthetic production occurs because each variable can be affected differently by a number of abiotic and biotic ecological factors, such as irradiance, temperature, desiccation, grazing, and resuspension (Coelho et al., 2009; Ubertini et al., 2012; Pratt et al., 2015; Savelli et al., 2018), leading to complex site-dependent interactions.

4.4 Inorganic nitrogen concentration in the water column and sediment

Dissolved inorganic nitrogen (DIN = NO_3^- + NO_2^- + NH_4^+) in the water column of the Guadalquivir Estuary was dominated by NO_3^-, >99% of DIN in February (Figure 4; Table 1). Similarly high concentrations of NO_3^- have been recorded in previous studies in the Guadalquivir Estuary and are likely associated with the nitrification of urban waste and runoff of excess fertilizers from agricultural fields (Mendiguchía et al., 2007; Flecha et al., 2015). Water column NO_3^- followed a seasonal change with maximum concentration in winter and minimum in summer, suggesting a link to the precipitation seasonal changes in the area (Figure 4; Supplementary Figure S1) and an important impact of fertilizers runoff from agricultural lands. NO_2^- and NH_4^+ changed clearly along the year but followed only partially the trend of NO_3^-, with low concentrations also observed in winter (Figure 4). The high concentration of water column NO_3^- does not sustain a correspondently high phytoplankton primary production due to light limitation due to the high turbidity (Supplementary Figure S1C) (Ruiz et al., 2017). Alternatively, PO_4^{3-} limitation could also contribute to explaining the low productivity due to the very high DIN : PO_4^{3-} ratio (Table 1). However, MPB biomass estimated by Chla was positively correlated with water column nitrate indicating that intertidal MPB could have a competitive ecological advantage over phytoplankton in turbid tidal estuaries, because at low tide MPB can receive sunlight directly (Underwood and Kromkamp, 1999).

Porewater NH_4^+, NO_3^-, and NO_2^- showed seasonal differences in both sampling sites although their time evolution was not always parallel (Figure 5). The range of porewater NH_4^+ and NO_2^- concentrations in the sediments of Guadalquivir Estuary was similar to those of other intertidal environments like the Bay of Cadiz (Garcia-Robledo et al., 2016; Haro et al., 2020), Tagus Estuary (Cabrita and Brotas, 2000), and the Eastern Scheldt (Rios-Yunes et al., 2023). In contrast, NO_3^- concentrations in the Guadalquivir estuary were an order of magnitude higher than those in the Bay of Cadiz and other environments (Cabrita and Brotas, 2000; Garcia-Robledo et al., 2016; Haro et al., 2020; Rios-Yunes et al., 2023), probably caused by the much higher NO_3^- concentration in the water column of the river. The vertical distribution of NH_4^+, NO_3^-, and NO_2^- followed the expected pattern in sediments (Berg et al., 1998, 2003). In the anoxic layers of sediment, NO_3^- and NO_2^- are used in denitrification and anammox contributing to the mineralization of organic matter under anoxic conditions (Hensen et al., 2006; Stein and Klotz, 2016). It is interesting to note that both inorganic nitrogen species in the sediment followed similar vertical distributions and seasonal trends (r = 0.65, $p < 0.05$, n = 100). In addition, NO_3^- and NO_2^- followed similar patterns in the porewater and the water column, evidencing a clear coupling between both compartments.

Vertical distribution of porewater NH_4^+ showed an inverse pattern to that of oxidized inorganic nitrogen species (Supplementary Figure S2; Figure 5), increasing downward as it is typically observed in marine sediments (Berg et al., 1998, 2003). The accumulation of porewater NH_4^+ is mainly the result of the progressive mineralization of organic matter, resulting in a long-term difussive efflux to the water column (Hensen et al., 2006). Nonetheless, this NH_4^+ flux to upper sediment layers and to the water column can be intercepted by different microbial communities. MPB can use directly NH_4^+ to fulfill its N demand for growth, a process energetically more favorable than the uptake

of NO_3^- and NO_2^-, which requires further reduction intracellularly (Dortch, 1990; Glibert et al., 2016). In addition, NH_4^+ in the oxic sediment layer serves as a substrate for nitrification and indirectly for coupled nitrification denitrification (Risgaard-Petersen, 2003). The seasonal trend of porewater NH_4^+ showed a maximum in August in both sampling locations, which might be related to a general stimulation of microbial degradation of organic matter by the higher summer temperatures.

4.5 Fluxes of inorganic nitrogen at sediment–water interface

Net fluxes of the different DIN species confirmed the important biogeochemical role of NO_3^- in this estuary. NO_3^- fluxes across the sediment–water interface were an order of magnitude higher than those of NH_4^+ and NO_2^-. Although occasionally a net NO_3^- efflux from the sediment toward the water column was recorded, on an annual average, the sediment was a net NO_3^- sink in both light and dark conditions (−0.70 ± 1.1 mmol NO_3^- m^2 h^{-1}). The magnitude of NO_3^- fluxes in the intertidal sediments of Guadalquivir Estuary were higher than those typically measured in subtidal sediments (Boynton et al., 2018, 2023; Rios-Yunes et al., 2023) and in intertidal sediments of different ecosystems (Bartoli et al., 2003; Rios-Yunes et al., 2023) but did not reach the very high values reported in the Tagus Estuary (Cabrita and Brotas, 2000). Net NH_4^+ fluxes in most of the incubations in both sampling sites along the year were close to zero or negative, indicating mainly a net NH_4^+ uptake by the sediment, same as NO_3^-. The overall magnitude of these NH_4^+ fluxes was similar to those found elsewhere, including intertidal sediments (Cabrita and Brotas, 2000; Bartoli et al., 2003; Rios-Yunes et al., 2023) and subtidal sediments where fluxes are usually positive, releasing NH_4^+ to the water column (Boynton et al., 2018, 2023). In addition to a dilution effect due to tidal mixing, the uptake of NH_4^+ and mainly NO_3^- by the Guadalquivir Estuary sediments likely contributes to the observed seaward reduction of water column concentrations of these nutrients (Mendiguchía et al., 2007; Flecha et al., 2015). Therefore, sediments have an important role buffering the high load of DIN from the water column and reducing its export to the Gulf of Cádiz.

MPB can consume NO_3^- and NH_4^+ for growth, therefore affecting their net fluxes at the sediment–water interface. The N demand of MPB can be estimated from the NCP rate using a photosynthetic quotient (0.9 CO_2:O_2, mol:mol) and the stoichiometric C:N ratio of MPB [119C:17N, mol:mol; (Hillebrand and Sommer, 1999)]. The mean NCP rates at Bonanza and Lebrija sites, 5.42 ± 2.02 mmol O_2 m^{-2} h^{-1} and 1.60 ± 1.85 mmol O_2 m^{-2} h^{-1}, represent an estimated N demand of 0.70 ± 0.26 mmol N m^{-2} h^{-1} and 0.20 ± 0.24 mmol N m^{-2} h^{-1}, in Bonanza and Lebrija, respectively. The mean annual DIN fluxes (J-NO_3^- + J-NO_2^- + J-NH_4^+) at the sediment water interface were −0.62 and −0.93 mmol N m^{-2} h^{-1}, in Bonanza and Lebrija, respectively. The MPB N-demand could account for the entire sediment DIN uptake in Bonanza and 21% in Lebrija. These calculations point out a relevant role of MPB as a potential N sink, particularly in Bonanza, affecting the exchange of DIN between the water column and sediments in the Guadalquivir Estuary, as shown elsewhere (Sundbäck et al., 2000; Risgaard-Petersen, 2003).

The differences in the net NO_3^- and NH_4^+ fluxes between light and dark conditions suggest a different role of MPB in the net sediment uptake of these nutrients from the water column. In general, the net sediment uptake rate of NH_4^+ was higher in light (−0.25 ± 0.38 and −0.05 ± 0.11 mmol NH_4^+ m^{-2} h^{-1} for Bonanza and Lebrija, respectively) than in darkness (0.01 ± 0.27 mmol NH_4^+ m^{-2} h^{-1} and −0.03 ± 0.04 mmol NH_4^+ m^{-2} h^{-1} for Bonanza and Lebrija), whereas no significant differences were found for net NO_3^- fluxes. The higher net NH_4^+ uptake rate in light is consistent with the expected higher N demand of MPB coupled to the photosynthetic activity and growth during light (Longphuirt et al., 2009) and the preference over NO_3^- during assimilation mentioned earlier. MPB used most likely a higher fraction of NH_4^+ from the water column in Bonanza compared with Lebrija, since the differences in net uptake rate between light and dark conditions and the N demand were higher in the former. The observation that the net NO_3^- uptake by the sediment did not change with light does not necessarily mean that MPB did not use water column NO_3^- at all, but rather that other processes, not light-dependent, might account for a larger fraction of the measured net NO_3^- fluxes. In fact, since the sum of the sediment net NH_4^+ uptake plus NH_4^+ production within the sediment is lower than that of MPB N-demand, the consumption of NO_3^- by MPB, despite being energetically less favorable, seems necessary. As far as the other processes are concerned, a substantial fraction of sediment NO_3^- uptake from the water column is likely due to high rates of denitrification in the anoxic sediment layer. These were probably higher in Lebrija than in Bonanza as suggested by a considerably higher net NO_3^- uptake in Lebrija and the evident excess of uptake compared with the estimated MPB N demand at this sampling location.

4.6 Iron and sulfate as alternative electrons acceptors

Porewater concentrations of Fe^{2+} and SO_4^{2-} were measured in the intertidal sediments of the Guadalquivir Estuary as an initial evaluation of the potential role of $Fe^{(III)}$ minerals and SO_4^{2-} as potential e^- acceptors for the microbial degradation of organic matter in anoxic conditions. The reduction of $Fe^{(III)}$ in the sediment releases Fe^{2+} that is soluble in anoxic conditions. Fe^{2+} concentrations in general were in the range of values reported for other estuaries (Pastor et al., 2011), being clearly higher in the most marine station of Bonanza (Supplementary Figure S2; Figure 6). They changed considerably with depth and season, with a characteristic peak at the 1.5-cm–2.5-cm depth in both sampling stations. The intensity of the subsurface peak changed seasonally, being clearly higher in summer in both sampling sites, coincident with the highest temperature and lowest nitrate concentration in the water column.

Integrated Fe^{2+} production rates, calculated from the porewater profiles, showed a strong increase in August 2019 (Supplementary Figure S3), and in the range of previously reported values for marine sediments (Canfield et al., 1993). The higher Fe-reduction activity in summer was related most likely to the higher temperatures that would reduce oxygen solubility and increase microbial activity, both aerobic

and anaerobic. Sediment Fe^{2+} concentrations were negatively correlated with those of NO_3^- in the water column ($r = -0.83$, $p < 0.05$), suggesting a negative feedback between these two compounds. In August 2019, the decrease in the water column NO_3^- limited or reduced denitrification, most likely decreasing competition and thus permitting increased rates of iron respiration. Similarly, the higher Fe^{2+} concentrations measured in Bonanza with respect to Lebrija could also be related to the higher availability of NO_3^- in the upstream zones, favoring its use as an electron acceptor over iron, since it is more favorable energetically.

Sulfate reduction is the dominant microbial process for organic matter mineralization in anoxic marine sediments, where SO_4^{2-} acts as an terminal electron acceptor in anaerobic microbial respiratory chains (Jorgensen and Kasten, 2006). The evaluation of the role of SO_4^{2-} reduction in estuarine sediments is more complex due to differences in SO_4^{2-} concentration along the freshwater–seawater salinity gradient. Concentrations were lower in Lebrija than in Bonanza as expected by the differences in salinity (Supplementary Table S1). In the first 10 cm of the Guadalquivir estuary sediments, the typical decrease in the SO_4^{2-} concentration with depth caused by SO_4^{2-} reduction (Jorgensen and Kasten, 2006; Jørgensen et al., 2019) was not evident. This might indicate that SO_4^{2-} reduction is not a relevant pathway for the oxidation of organic matter in the upper sediment layers of the Guadalquivir estuary.

4.7 Mineralization of organic matter in the sediment

The mineralization of organic matter in the sediment occurs by aerobic respiration in the oxic upper sediment layer, and a variety of anaerobic metabolic pathways below the oxic penetration depth (Middelburg et al., 1993). Dark respiration rate represents a good estimate of aerobic and anaerobic organic matter mineralization since it encompasses both the O_2 consumption in the direct oxidation of the organic compounds plus the O_2 being consumed in the reoxidation of reduced inorganic products produced during anaerobic degradation (NH_4^+, H_2S, Fe^{2+}, etc.) (Jorgensen et al., 2022). Thus, dark respiration rates were consistently higher in Bonanza sediments than in Lebrija, 2.38 ± 0.99 mmol m^{-2} h^{-1} and 1.32 ± 0.29 mmol m^{-2} h^{-1}, corresponding to C_{org} mineralization rates of 2.14 ± 0.89 mmol CO_2 m^{-2} h^{-1} and 1.19 ± 0.26 mmol CO_2 m^{-2} h^{-1}, respectively (Table 2), using a respiratory quotient of CO_2:O_2 = 0.90 (Jorgensen et al., 2022).

The shape of DIC profiles indicates the existence of an upward DIC flux, as a result of organic matter mineralization. In light, part of the CO_2 upward flux to the water column can be intercepted by the photosynthetic C-fixation activity of MPB (Sundbäck et al., 2004). Net DIC production ranged from 0.30 ± 0.05 mmol m^{-2} h^{-1} to 1.29 ± 0.14 to mmol m^{-2} h^{-1} in Bonanza, and from 0.36 ± 0.09 mmol m^{-2} h^{-1} to 0.94 ± 0.47 mmol m^{-2} h^{-1} in Lebrija (Supplementary Figure S3D; Table 2). These rates, determined by modeling DIC profiles (Berg et al., 1998), were lower (38%–69%) than the C_{org} mineralization rates calculated from the O_2 consumption rates in darkness. Nonetheless, they confirmed a higher annual mean mineralization rate in Bonanza than in Lebrija. Methodological differences inherent to both approaches and the consumption of a fraction of CO_2 produced within the sediment by MPB photosynthetic C fixation might explain the lower mineralization rates estimated from the steady-state DIC profiles.

Net NH_4^+ mineralization rates were consistently higher in Lebrija than in Bonanza throughout the year, showing in both sites parallel seasonal changes that were not observed in other biogeochemical variables (Supplementary Figure S3; Table 2). Using the mean C:N stoichiometry for both sites, 15.4 and 12.2 for Bonanza and Lebrija sediments, respectively, the annual mean NH_4^+ production rates were converted to C_{org} units, resulting in 0.16 ± 0.11 mmol CO_2 m^{-2} h^{-1} and 0.32 ± 0.07 mmol CO_2 m^{-2} h^{-1}. These rates of organic matter mineralization estimated from NH_4^+ profiles were only 20% and 50%

TABLE 2 Sediment net community production and organic matter mineralization rates averaged for the period of study (n = 5, mean ± SD) at each of the two locations studied in the Guadalquivir estuary.

	Process rates (mmol m^{-2} h^{-1})		Source of data	Estimation of C_{org} fixation and mineralization rates (mmol CO_2 m^{-2} h^{-1})	
	Bonanza	Lebrija		Bonanza	Lebrija
Net community production (NCP)*	5.42 ± 2.02	1.60 ± 1.85	Core incubations	4.88 ± 1.82	1.44 ± 1.67
Dark respiration (R_{dark})	2.38 ± 0.99	1.32 ± 0.29	Core incubations	2.14 ± 0.11	1.19 ± 0.26
Net DIC production	0.82 ± 0.36	0.64 ± 0.19	Porewater profiles	0.82 ± 0.36	0.64 ± 0.19
Net NH_4^+ production*	0.011 ± 0.007	0.026 ± 0.006	Porewater profiles	0.16 ± 0.11	0.32 ± 0.07
Net Fe^{2+} production	0.05 ± 0.06	0.02 ± 0.03	Porewater profiles	0.012 ± 0.015	0.005 ± 0.007
Net SO_4^{2-} reduction	0.005 ± 0.006	0.001 ± 0.001	Porewater profiles	0.010 ± 0.012	0.002 ± 0.002
Net NO_3^- reduction	0.52 ± 1.04	0.89 ± 1.06	Core incubations	0.64 ± 1.30	1.12 ± 1.33
Net CH_4 production	0.0004–0.0008	0.002–0.004	Sánchez-Rodríguez et al. (2022)	0.0008–0.0016	0.004–0.008

Photosynthetic quotient used for NCP in light and respiratory quotient for dark respiration were 0.9 in both cases. Stoichiometric ratios for converting measured rates to C units were: 106C:424Fe^{2+}; 106C:53SO_4^{2-}; 106C:84.8NO_3^-; 106C:53CH_4 (Froelich et al., 1979). Net NO_3^- reduction (denitrification) was calculated from the net sediment NO_3^- uptake from the water column in darkness. Net CH_4 production rates (methanogenesis) have been taken from Sánchez-Rodríguez et al. (2022). * indicates that there is a statistically clear difference between Bonanza and Lebrija (T-test, statistical significance p-value <0.05).

of those calculated from the DIC profiles for Bonanza and Lebrija respectively. NH_4^+ from mineralization of organic matter can be quickly used for nitrification and as a source of N for MPB (Sundbäck et al., 2000; Risgaard-Petersen, 2003; Glibert et al., 2016), reducing thus the NH_4^+ accumulation within the sediment and resulting in the underestimation of the mineralization rates. In addition, in muddy sediments, the adsorption of NH_4^+ to the sediment particles, not measured here, can represent a significant fraction of the total NH_4^+ pool (Mackin and Aller, 1984), likely resulting in further underestimating the NH_4^+ production in the sediment.

The potential contributions of the reduction of iron oxides (Fe^{III}) and SO_4^{2-} as terminal e^- acceptors for the mineralization of organic matter can be calculated using suitable stoichiometric ratios (Froelich et al., 1979). These calculations for the Guadalquivir Estuary sediments suggest a relatively minor quantitative role for these two anaerobic microbial pathways (Table 2). In both cases, estimated mean annual rates were up to two orders of magnitude lower than aerobic rates estimated as oxygen consumption rates. Although not measured in our study, methanogenesis is typically high in estuarine sediments, contributing to the degradation of OM in anoxic conditions (Zhou et al., 2009; Wells et al., 2020). Benthic methane fluxes in subtidal sediments of the Guadalquivir Estuary decreased seaward, with rates of approximately 0.4–0.8 μmol CH_4 m^{-2} h^{-1} and 2.0–4.0 μmol CH_4 m^{-2} h^{-1}, in Bonanza and Lebrija, respectively (Sánchez-Rodríguez et al., 2022) (Table 2). Even taking into account that these release rates likely underestimated the actual CH_4 production rate due to aerobic and anaerobic CH_4 oxidation within the sediment (Myllykangas et al., 2020; Abril and Iversen, 2002), they represent a very small contribution to the oxidation of organic matter in the Guadalquivir Estuary sediments in anoxic conditions, much lower than Fe^{III} reduction and SO_4^{2-} reduction (Table 2).

In contrast, denitrification might have a relevant role in the mineralization of organic matter in the Guadalquivir Estuary due to the high NO_3^- content in the water column. The denitrification rate can be estimated from the net NO_3^- uptake rate of the sediment in darkness, producing rates of 0.71 ± 0.57 mmol NO_3^- m^{-2} h^{-1} and 0.97 ± 1.23 mmol NO_3^- m^{-2} h^{-1} in Bonanza and Lebrija, respectively (Table 2). When denitrification rates were transformed to C units using a suitable stoichiometric ratio for denitrification (Froelich et al., 1979), the results clearly showed a strong contribution of this process, varying between 30% and 94% of the values for dark O_2 respiration. Denitrification was also more than an order of magnitude higher than the contributions estimated for net Fe^{III} and SO_4^{2-} reduction and methanogenesis in the sediments of the Guadalquivir Estuary (Table 2). These results point out to the potential importance of denitrification in the oxidation of organic matter in the anoxic sediments of the Guadalquivir Estuary.

5 Conclusion

The estuary of the Guadalquivir River, in addition to its high turbidity, is characterized by very high NO_3^- concentrations in the water column. This study shows for the first time that the high NO_3^- concentration and the presence of intertidal MPB as benthic primary producers in the riverbanks condition strongly the C and N biogeochemical cycling at the sediment–water interface. Net community production of intertidal sediments was generally positive due to the MPB photosynthetic activity, making the sediment net autotrophic and contributing positively to the overall autochthonous primary production of the estuary. The high NO_3^- concentration in the water column is a very strong determinant of sediment biogeochemistry in this estuary. NO_3^- fluxes dominated the exchange of DIN between the sediment and the water column, with sediments being a net sink of NO_3^- and NH_4^+, therefore reducing the export of DIN to the Gulf of Cádiz. The estimated N demand of MPB in Bonanza was slightly higher than the total DIN net uptake, whereas in Lebrija, it represented 21% of the total. This suggests that the MPB can have a potential strong impact on NO_3^- and NH_4^+ net fluxes between the water column and the sediment. On the one hand, the significantly higher sediment uptake of NH_4^+ in light with respect to dark conditions, a pattern not observed for NO_3^-, seems to suggest that the majority of MPB N demand is satisfied by the uptake of NH_4^+ from the water column. On the other hand, the high concentration of water column NO_3^-, in addition to supporting partially the MPB N demand, likely sustained high rates of denitrification within the sediment. Water column-dependent denitrification seems to be the most important anaerobic pathway for the oxidation of organic matter, surpassing Fe reduction, SO_4^{2-} reduction and methanogenesis by several orders of magnitude. Direct measurement of these microbial processes and the identification of the microorganisms involved by metagenomics are evident next steps to understand better the biogeochemical cycling of C and N in the Guadalquivir Estuary.

Data availability statement

The raw data supporting the conclusions of this article will be made available by the authors, without undue reservation.

Author contributions

VP: Conceptualization, Data curation, Formal analysis, Investigation, Software, Visualization, Writing – original draft, Writing – review & editing. AC: Conceptualization, Data curation, Funding acquisition, Formal analysis, Methodology, Resources, Validation, Writing - original draft, Writing – review & editing. SP: Conceptualization, Formal analysis, Funding acquisition, Methodology, Resources, Software, Validation, Writing – review & editing. SB: Investigation, Data curation, Methodology, Writing - review & editing. CV: Conceptualization, Investigation, Resources, Writing - review & editing. JPC: Investigation, Funding acquisition, Resources, Writing - review & editing. EG: Conceptualization, Data curation, Funding acquisition, Investigation, Methodology, Project administration, Resources, Software, Supervision, Validation, Writing – review & editing.

Funding

The author(s) declare financial support was received for the research, authorship, and/or publication of this article. This work has been funded by the project FEDER-UCA18–107225 from the 2014–2020 ERDF Operational Program and by the Department of Economy,

Knowledge, Business and University of the Regional Government of Andalusia; the project CTM2017–82274-R from the Ministry of Economy, Industry and Competitiveness of the Government of Spain; and GUADACONECT, PP.FEM.PPA201900.005. Open access fee was co-funded by the QUALIFICA Project (QUAL21–0019, Junta de Andalucía) and the Internal Research Program of the University of Cadiz (Plan Propio - UCA 2023–2024). EGR was funded by the Ramon y Cajal Program, reference RYC2019-027675-I.

Conflict of interest

The authors declare that the research was conducted in the absence of any commercial or financial relationships that could be construed as a potential conflict of interest.

Publisher's note

Supplementary material

The Supplementary Material for this article can be found online at: https://www.frontiersin.org/articles/10.3389/fmars.2024.1389673/full#supplementary-material

References

Abril, G., and Iversen, N. (2002). Methane dynamics in a shallow non-tidal estuary (Randers Fjord, Denmark). *Mar. Ecol. Prog. Ser.* 230, 171–181. doi: 10.3354/meps230171

Anderson, M. J., Gorley, R. N., and Clarke, K. R. (2008). *PERMANOVA + for PRIMER: Guide to Software and Statistical Methods* (Plymouth, UK: PRIMER-E).

Bartoli, M., Nizzoli, D., and Viaroli, P. (2003). Microphytobenthos activity and fluxes at the sediment-water interface: Interactions and spatial variability. *Aquat. Ecol.* 37, 341–349. doi: 10.1023/B:AECO.0000007040.43077.5f

Berg, P., Risgaard-Petersen, N., and Rysgaard, S. (1998). Interpretation of measured concentration profiles in sediment pore water. *Limnol. Ocean.* 43, 1500–1510. doi: 10.4319/lo.1998.43.7.1500

Berg, P., Rysgaard, S., and Thamdrup, B. (2003). Dynamic modeling of early diagenesis and nutrient cycling. A case study in an arctic marine sediment. *Am. J. Sci.* 303, 905–955. doi: 10.2475/ajs.303.10.905

Bohórquez, J., Calenti, D., García-Robledo, E., Papaspyrou, S., Jimenez-Arias, J. L., Gómez-Ramírez, E. H., et al. (2019). Water column dissolved silica concentration limits microphytobenthic primary production in intertidal sediments. *J. Phycol.* 55, 625–636. doi: 10.1111/jpy.12838

Bohórquez, J., McGenity, T. J., Papaspyrou, S., García-Robledo, E., Corzo, A., and Underwood, G. J. C. (2017). Different types of diatom-derived extracellular polymeric substances drive changes in heterotrophic bacterial communities from intertidal sediments. *Front. Microbiol.* 8. doi: 10.3389/fmicb.2017.00245

Bower, C. E., and Holm-Hansen, T. (1980). A salicylate–hypochlorite method for determining ammonia in seawater. *Can. J. Fish. Aquat. Sci.* 37, 794–798. doi: 10.1139/f80-106

Boynton, W. R., Ceballos, M. A. C., Bailey, E. M., Hodgkins, C. L. S., Humphrey, J. L., and Testa, J. M. (2018). Oxygen and nutrient exchanges at the sediment-water interface: a global synthesis and critique of estuarine and coastal data. *Estuaries Coasts* 41, 301–333. doi: 10.1007/s12237-017-0275-5

Boynton, W. R., Ceballos, M. A. C., Hodgkins, C. L. S., Liang, D., and Testa, J. M. (2023). Large-scale spatial and temporal patterns and importance of sediment–water oxygen and nutrient fluxes in the Chesapeake Bay region. *Estuaries Coasts* 46, 356–375. doi: 10.1007/s12237-022-01127-0

Burgos, M., Ortega, T., Bohórquez, J., Corzo, A., Rabouille, C., and Forja, J. M. (2018a). Seasonal variation of early diagenesis and greenhouse gas production in coastal sediments of Cadiz Bay: Influence of anthropogenic activities. *Estuar. Coast. Shelf Sci.* 200, 99–115. doi: 10.1016/j.ecss.2017.10.016

Burgos, M., Ortega, T., and Forja, J. (2018b). Carbon dioxide and methane dynamics in three coastal systems of Cadiz Bay (SW Spain). *Estuaries Coasts* 41, 1069–1088. doi: 10.1007/s12237-017-0330-2

Cabrita, M. T., and Brotas, V. (2000). Seasonal variation in denitrification and dissolved nitrogen fluxes in intertidal sediments of the Tagus estuary, Portugal. *Mar. Ecol. Prog. Ser.* 202, 51–65. doi: 10.3354/meps202051

Canfield, D. E., Jorgensen, B. B., Fossing, H., Glud, R., Gundersen, J., Ramsing, N. B., et al. (1993). Pathways of organic carbon oxidation in three continental margin sediments. *Mar. Geol.* 113, 27–40. doi: 10.1016/0025-3227(93)90147-N

Canfield, D. E., Thamdrup, B., and Kristensen, E. (2005). Aquatic Geomicrobiology. *Advances in Marine Biology*, (Elsevier: Academic Press) , 1-642. doi: 10.1016/S0065-2881(05)48017-7

Coelho, H., Vieira, S., and Serôdio, J. (2009). Effects of desiccation on the photosynthetic activity of intertidal microphytobenthos biofilms as studied by optical methods. *J. Exp. Mar. Bio. Ecol.* 381, 98–104. doi: 10.1016/j.jembe.2009.09.013

Corzo, A., Van Bergeijk, S. A., and García-Robledo, E. (2009). Effects of green macroalgal blooms on intertidal sediments: net metabolism and carbon and nitrogen contents. *Mar. Ecol. Prog. Ser.* 380, 81–93. doi: 10.3354/meps07923

Díez-Minguito, M., Baquerizo, A., Ortega-Sánchez, M., Navarro, G., and Losada, M. A. (2012). Tide transformation in the Guadalquivir estuary (SW Spain) and process-based zonation. *J. Geophys. Res. Ocean.* 117, 1–14. doi: 10.1029/2011JC007344

Díez-Minguito, M., and de Swart, H. E. (2020). Relationships between chlorophyll-a and suspended sediment concentration in a high-nutrient load estuary: an observational and idealized modeling approach. *J. Geophys. Res. Ocean.* 125, e2019JC015188. doi: 10.1029/2019JC015188

Donázar-Aramendía, I., Sánchez-Moyano, J. E., García-Asencio, I., Miró, J. M., Megina, C., and García-Gómez, J. C. (2019). Human pressures on two estuaries of the Iberian Peninsula are reflected in food web structure. *Sci. Rep.* 9, 1–10. doi: 10.1038/s41598-019-47793-2

Dortch, Q. (1990). The interaction between ammonium and nitrate uptake in phytoplankton. *Mar. Ecol. Prog. Ser.* 61, 183–201. doi: 10.3354/meps061183

Dushoff, J., Kain, M. P., and Bolker, B. M. (2019). I can see clearly now: Reinterpreting statistical significance. *Methods Ecol. Evol.* 10, 756–759. doi: 10.1111/2041-210X.13159

Flecha, S., Huertas, I. E., Navarro, G., Morris, E. P., and Ruiz, J. (2015). Air–water CO2 fluxes in a highly heterotrophic estuary. *Estuaries Coasts* 38, 2295–2309. doi: 10.1007/s12237-014-9923-1

Froelich, P. N., Klinkhammer, G. P., Bender, M. L., Luedtke, N. A., Heath, G. R., Cullen, D., et al. (1979). Early oxidation of organic matter in pelagic sediments of the eastern equatorial Atlantic: suboxic diagenesis. *Geochim. Cosmochim. Acta* 43, 1075–1090. doi: 10.1016/0016-7037(79)90095-4

Garcia-Robledo, E., Bohorquez, J., Corzo, A., Jimenez-Arias, J. L., and Papaspyrou, S. (2016). Dynamics of inorganic nutrients in intertidal sediments: Porewater, exchangeable, and intracellular pools. *Front. Microbiol.* 7. doi: 10.3389/fmicb.2016.00761

García-Robledo, E., Corzo, A., and Papaspyrou, S. (2014). A fast and direct spectrophotometric method for the sequential determination of nitrate and nitrite at low concentrations in small volumes. *Mar. Chem.* 162, 30–36. doi: 10.1016/j.marchem.2014.03.002

García-Robledo, E., Corzo, A., Papaspyrou, S., Jiménez-Arias, J. L., and Villahermosa, D. (2010). Freeze-lysable inorganic nutrients in intertidal sediments: Dependence on microphytobenthos abundance. *Mar. Ecol. Prog. Ser.* 403, 155–163. doi: 10.3354/meps08470

Glibert, P. M., Wilkerson, F. P., Dugdale, R. C., Raven, J. A., Dupont, C. L., Leavitt, P. R., et al. (2016). Pluses and minuses of ammonium and nitrate uptake and assimilation by phytoplankton and implications for productivity and community composition, with emphasis on nitrogen-enriched conditions. *Limnol. Oceanogr.* 61, 165–197. doi: 10.1002/lno.10203

Grasshoff, K., Kremling, K., and Ehrhardt, M. (1999). *Methods of seawater analysis. 3rd ed.* Ed. (Weinheim, New York, Chiester, Brisbane, Singopore: WILEY-VCH). doi: 10.1016/0304-4203(78)90045-2

Haro, S., Bohórquez, J., Lara, M., Garcia-Robledo, E., González, C. J., Crespo, J. M., et al. (2019). Diel patterns of microphytobenthic primary production in intertidal sediments: the role of photoperiod on the vertical migration circadian rhythm. *Sci. Rep.* 9, 13376. doi: 10.1038/s41598-019-49971-8

Haro, S., Jesus, B., Oiry, S., Papaspyrou, S., Lara, M., González, C. J., et al. (2022). Microphytobenthos spatio-temporal dynamics across an intertidal gradient using Random Forest classification and Sentinel-2 imagery. *Sci. Total Environ.* 804, 149983. doi: 10.1016/j.scitotenv.2021.149983

Haro, S., Lara, M., Laiz, I., González, C. J., Bohórquez, J., Garcia-Robledo, E., et al. (2020). Microbenthic net metabolism along intertidal gradients (Cadiz bay, SW Spain): spatio-temporal patterns and environmental factors. *Front. Mar. Sci.* 7. doi: 10.3389/fmars.2020.00039

Hedges, J. I., Keil, R. G., and Benner, R. (1997). What happens to terrestrial organic matter in the ocean? *Org. Geochem.* 27, 195–212. doi: 10.1016/S0146-6380(97)00066-1

Hensen, C., Zabel, M., and Schulz, H. N. (2006). "Benthic cycling of oxygen, nitrogen and phosphorus," in *Marine Geochemistry* (Berlin, Heidelberg: Springer), 207–240. doi: 10.1007/3-540-32144-6_6

Hillebrand, H., and Sommer, U. (1999). The nutrient stoichiometry of benthic microalgal growth: Redfield proportions are optimal. *Limnol. Oceanogr.* 44, 440–446. doi: 10.4319/lo.1999.44.2.0440

Høgslund, S., Fossing, H., and Carstensen, J. (2023). Microphytobenthic impact on benthic pelagic nutrient exchange in temperate shallow estuaries. *Estuar. Coast. Shelf Sci.* 292, 108475. doi: 10.1016/j.ecss.2023.108475

Huertas, I. E., Flecha, S., Navarro, G., Perez, F. F., and de la Paz, M. (2018). Spatio-temporal variability and controls on methane and nitrous oxide in the Guadalquivir Estuary, Southwestern Europe. *Aquat. Sci.* 80, 29. doi: 10.1007/s00027-018-0580-5

Jørgensen, B. B., Findlay, A. J., and Pellerin, A. (2019). The biogeochemical sulfur cycle of marine sediments. *Front. Microbiol.* 10. doi: 10.3389/fmicb.2019.00849

Jorgensen, B. B., and Kasten, (2006). "Sulfur cycling and methane oxidation," in *Marine Geochemistry* (Berlin, Heidelberg: Springer), 371–427. doi: 10.1007/3-540-32144-6_11

Jorgensen, B. B., Wenzhöfer, F., Egger, M., and Glud, R. N. (2022). Sediment oxygen consumption: Role in the global marine carbon cycle. *Earth-Science Rev.* 228, 103987. doi: 10.1016/j.earscirev.2022.103987

Kwon, B. O., Kim, H., Noh, J., Lee, S. Y., Nam, J., and Khim, J. S. (2020). Spatiotemporal variability in microphytobenthic primary production across bare intertidal flat, saltmarsh, and mangrove forest of Asia and Australia. *Mar. pollut. Bull.* 151, 110707. doi: 10.1016/j.marpolbul.2019.110707

Lee, C., Wakeham, S. G., and XXXI. Hedges, J. (2000). Composition and flux of particulate amino acids and chloropigments in equatorial Pacific seawater and sediments. *Deep. Res. Part I Oceanogr. Res. Pap.* 47, 1535–1568. doi: 10.1016/S0967-0637(99)00116-8

Li, Y. H., and Gregory, S. (1974). Diffusion of ions in sea water and in deep-sea sediments. Geochim. Cosmochim. Acta. *Geochim. Cosmochim. Acta* 38, 703–714. doi: 10.1016/0016-7037(74)90145-8

Longphuirt, S. N., Lim, J. H., Leynaert, A., Claquin, P., Choy, E. J., Kang, C. K., et al. (2009). Dissolved inorganic nitrogen uptake by intertidal microphytobenthos: Nutrient concentrations, light availability and migration. *Mar. Ecol. Prog. Ser.* 379, 33–44. doi: 10.3354/meps07852

Macintyre, H. L., Geider, R. J., and Miller, D. C. (1996). Microphytobenthos: The ecological role of the "secret garden" of unvegetated, shallow-water marine habitats. I. Distribution, abundance and primary production. *Estuaries* 19, 186–201. doi: 10.2307/1352224

Mackin, J. E., and Aller, R. C. (1984). Ammonium adsorption in marine sediments. *Limnol. Oceanogr.* 29, 250–257. doi: 10.4319/lo.1984.29.2.0250

McTigue, N. D., Bucolo, P., Liu, Z., and Dunton, K. H. (2015). Pelagic-benthic coupling, food webs, and organic matter degradation in the Chukchi Sea: Insights from sedimentary pigments and stable carbon isotopes. *Limnol. Oceanogr.* 60, 429–445. doi: 10.1002/lno.10038

Megina, C., Donázar-Aramedía, Í., Miró, J. M., García-Lafuente, J., and García-Gómez, J. C. (2023). The hyperturbid mesotidal Guadalquivir estuary during an extreme turbidity event: Identifying potential management strategies. *Ocean Coast. Manage.* 246. doi: 10.1016/j.ocecoaman.2023.106903

Mendiguchía, C., Moreno, C., and García-Vargas, M. (2007). Evaluation of natural and anthropogenic influences on the Guadalquivir River (Spain) by dissolved heavy metals and nutrients. *Chemosphere* 69, 1509–1517. doi: 10.1016/j.chemosphere.2007.05.082

Middelburg, J. J., Barranguet, C., Boschker, H. T. S., Herman, P. M. J., Moens, T., and Heip, C. H. R. (2000). The fate of intertidal microphytobenthos carbon: An in *situ* 13C-labeling study. *Limnol. Oceanogr.* 45, 1224–1234. doi: 10.4319/lo.2000.45.6.1224

Middelburg, J. J., Vlug, T., and van der Nat, J. W. A. (1993). Organic matter mineralization in marine systems. *Glob. Planet. Change* 8, 47–58. doi: 10.1016/0921-8181(93)90062-S

Miró, J. M., Megina, C., Donázar-aramendía, I., and García-gómez, J. C. (2022). Effects of maintenance dredging on the macrofauna of the water column in a turbid estuary. *Sci. Total Environ.* 806. doi: 10.1016/j.scitotenv.2021.151304

Miró, J. M., Megina, C., Donázar-Aramendía, I., Reyes-Martínez, M. J., Sánchez-Moyano, J. E., and García-Gómez, J. C. (2020). Environmental factors affecting the nursery function for fish in the main estuaries of the Gulf of Cadiz (south-west Iberian Peninsula). *Sci. Total Environ.* 737, 139614. doi: 10.1016/j.scitotenv.2020.139614

Myllykangas, J. P., Rissanen, A. J., Hietanen, S., and Jilbert, T. (2020). Influence of electron acceptor availability and microbial community structure on sedimentary methane oxidation in a boreal estuary. *Biogeochemistry* 148, 291–309. doi: 10.1007/s10533-020-00660-z

Navarro, G., Gutiérrez, F. J., Díez-Minguito, M., Losada, M. A., and Ruiz, J. (2011). Temporal and spatial variability in the Guadalquivir estuary: A challenge for real-time telemetry. *Ocean Dyn.* 61, 753–765. doi: 10.1007/s10236-011-0379-6

Pastor, L., Cathalot, C., Deflandre, B., Viollier, E., Soetaert, K., Meysman, F. J. R., et al. (2011). Modeling biogeochemical processes in sediments from the Rhône River prodelta area (NW Mediterranean Sea). *Biogeosciences* 8, 1351–1366. doi: 10.5194/bg-8-1351-2011

Paterson, D. M. (1989). Short-term changes in the erodibility of intertidal cohesive sediments related to the migratory behavior of epipelic diatoms. *Limnol. Oceanogr.* 34, 223–234. doi: 10.4319/lo.1989.34.1.0223

Pratt, D. R., Pilditch, C. A., Lohrer, A. M., Thrush, S. F., and Kraan, C. (2015). Spatial distributions of grazing activity and microphytobenthos reveal scale-dependent relationships across a sedimentary gradient. *Estuaries Coasts* 38, 722–734. doi: 10.1007/s12237-014-9857-7

Rios-Yunes, D., Tiano, J. C., van Oevelen, D., van Dalen, J., and Soetaert, K. (2023). Annual biogeochemical cycling in intertidal sediments of a restored estuary reveals dependence of N, P, C and Si cycles to temperature and water column properties. *Estuar. Coast. Shelf Sci.* 282, 108227. doi: 10.1016/j.ecss.2023.108227

Risgaard-Petersen, N. (2003). Coupled nitrification-denitrification in autotrophic and heterotrophic estuarine sediments: On the influence of benthic microalgae. *Limnol. Oceanogr.* 48, 93–105. doi: 10.4319/lo.2003.48.1.0093

Ruiz, J., Macías, D., and Navarro, G. (2017). Natural forcings on a transformed territory overshoot thresholds of primary productivity in the Guadalquivir estuary. *Cont. Shelf Res.* 148, 199–207. doi: 10.1016/j.csr.2017.09.002

Sánchez-Rodríguez, J., Sierra, A., Jiménez-López, D., Ortega, T., Gómez-Parra, A., and Forja, J. (2022). Dynamic of CO2, CH4 and N2O in the guadalquivir estuary. *Sci. Total Environ.* 805, 150193. doi: 10.1016/j.scitotenv.2021.150193

Sarazin, G., Michard, G., and Prevot, F. (1999). A rapid and accurate spectroscopic method for alkalinity measurements in sea water samples. *Water Res.* 33, 290–294. doi: 10.1016/S0043-1354(98)00168-7

Savelli, R., Dupuy, C., Barillé, L., Lerouxel, A., Guizien, K., Philippe, A., et al. (2018). On biotic and abiotic drivers of the microphytobenthos seasonal cycle in a temperate intertidal mudflat: A modelling study. *Biogeosciences* 15, 7243–7271. doi: 10.5194/bg-15-7243-2018

Schutte, C. A., Ahmerkamp, S., Wu, C. S., Seidel, M., De Beer, D., Cook, P. L. M., et al. (2018). "Chapter 12 - Biogeochemical dynamics of coastal tidal flats," in *Coastal Wetlands: An Integrated Ecosystem Approach* (Elsevier), 407–440. doi: 10.1016/B978-0-444-63893-9.00012-5

Soetaert, K., Middelburg, J. J., Heip, C., Meire, P., Van Damme, S., and Maris, T. (2006). Long-term change in dissolved inorganic nutrients in the heterotrophic Scheldt estuary (Belgium, The Netherlands). *Limnol. Oceanogr.* 51, 409–423. doi: 10.4319/lo.2006.51.1_part_2.0409

Stal, L. J., van Gemerden, H., and Krumbein, W. E. (1984). The simultaneous assay of chlorophyll and bacteriochlorophyll in natural microbial communities. *J. Microbiol. Methods* 2, 295–306. doi: 10.1016/0167-7012(84)90048-4

Stein, L. Y., and Klotz, M. G. (2016). The nitrogen cycle. *Curr. Biol.* 26, R94–R98. doi: 10.1016/j.cub.2015.12.021

Sundbäck, K., Linares, F., Larson, F., Wulff, A., and Engelsen, A. (2004). Benthic nitrogen fluxes along a depth gradient in a microtidal fjord: The role of denitrification and microphytobenthos. *Limnol. Oceanogr.* 49, 1095–1107. doi: 10.4319/lo.2004.49.4.1095

Sundbäck, K., and Miles, A. (2002). Role of microphytobenthos and denitrification for nutrient turnover in embayments with floating macroalgal mats: A spring situation. *Aquat. Microb. Ecol.* 30, 91–101. doi: 10.3354/ame030091

Sundbäck, K., Miles, A., and Göransson, E. (2000). Nitrogen fluxes, denitrification and the role of microphytobenthos in microtidal shallow-water sediments: An annual study. *Mar. Ecol. Prog. Ser.* 200, 59–76. doi: 10.3354/meps200059

Ubertini, M., Lefebvre, S., Gangnery, A., Grangeré, K., Le Gendre, R., and Orvain, F. (2012). Spatial variability of benthic-pelagic coupling in an estuary ecosystem: consequences for microphytobenthos resuspension phenomenon. *PLoS One* 7, e44155. doi: 10.1371/journal.pone.0044155

Underwood and Kromkamp (1999). Primary production by phytoplankton and microphytobenthos in estuaries. *Adv. Ecol. Res.* 29, 93–154. doi: 10.1016/s0065-2504(08)60192-0

Viollier, E., Inglett, P. W., Hunter, K., Roychoudhury, A. N., and van Cappellen, P. (2000). The Ferrozine method revisted. *Applied Geochemistry* 15, 6, 785–790. doi: 10.1016/S0883-2927(99)00097-9

Wells, N. S., Chen, J. J., Maher, D. T., Huang, P., Erler, D. V., Hipsey, M., et al. (2020). Changing sediment and surface water processes increase CH4 emissions from human-impacted estuaries. *Geochim. Cosmochim. Acta* 280, 130–147. doi: 10.1016/j.gca.2020.04.020

Yallop, M. L., De Winder, B., Paterson, D. M., and Stal, L. J. (1994). Comparative structure, primary production and biogenic stabilization of cohesive and non-cohesive marine sediments inhabited by microphytobenthos. *Estuar. Coast. Shelf Sci.* 39, 565–582. doi: 10.1016/S0272-7714(06)80010-7

Zhou, H., Yin, X., Yang, Q., Wang, H., Wu, Z., and Bao, S. (2009). Distribution, source and flux of methane in the western Pearl River Estuary and northern South China Sea. *Mar. Chem.* 117, 21–31. doi: 10.1016/j.marchem.2009.07.011

Zuur, A. F., Ieno, E. N., and Elphick, C. S. (2010). A protocol for data exploration to avoid common statistical problems. *Methods Ecol. Evol.* 1, 3–14. doi: 10.1111/j.2041-210X.2009.00001.x